Journal of ELECTRONIC MATERIALS, Vol. 41, No. 7, 2012
DOI: 10.1007/s11664-012-1980-2

Growth of CdS Nanoneedles by Pulsed Laser Deposition

LI CHEN,[1] XIAONIU FU,[1] JUSHUI LAI,[1] JIAN SUN,[1] ZHIFENG YING,[1] JIADA WU,[1] and NING XU[1,2]

1.—Key Laboratory for Micro and Nanophotonic Structures of Ministry of Education, Department of Optical Science and Engineering, Fudan University, Shanghai 200433, People's Republic of China. 2.—e-mail: ningxu@fudan.edu.cn

CdS nanoneedles have been grown on Ni-coated Si (100) substrates by pulsed laser deposition. Substrate temperature and Ni-catalyst layer thickness were found to have great effects on the density and morphology of the as-grown CdS nanoneedles. Crystalline CdS nanoneedles with middle diameter and length of about 40 nm to 100 nm and 400 nm to 1000 nm, respectively, could be obtained at 350°C to 450°C on Ni-coated silicon (100) substrates, and nanoneedles with good shapes were obtained at 400°C substrate temperature. From the cross-section morphologies, it was found that the CdS nanoneedles grew out of the base CdS crystallite layer with thickness of about 500 nm. Based on the experimental results, vapor–solid and vapor–liquid–solid growth modes describe the CdS nanoneedle growth.

Key words: CdS nanoneedles, pulsed laser deposition, Ni-catalyst

INTRODUCTION

CdS, one of the II–VI semiconductors, is a good and sensitive optoelectronic material with a wide direct band gap of 2.42 eV,[1,2] having potential applications in light-emitting diodes (LEDs),[3,4] light sensors,[5–7] photocatalysts,[8,9] and hybrid solar cells.[10] If nanostructures can be introduced into this material, the sensitivities and efficiencies of these devices could be greatly increased due to the increased specific surface area and quantum size effects. In recent years, methods of synthesis of CdS nanowires, such as electrochemical deposition,[11–13] solvothemal route,[14–16] and chemical or physical vapor deposition,[17,18] have been rapidly developed. Compared with these routes, pulsed laser deposition (PLD) is a relatively efficient and simple approach.[19] Using PLD, it is easy to control the growth process and avoid sample contamination because the laser-ablated plumes have good directionality and the surroundings are kept at low temperatures. Congruent ablation and very little contamination make PLD appropriate for synthesis of nanocrystals of refractory compounds such as CdS.[20,21] Moreover, the considerable kinetic energies of the laser-ablated species enable them to migrate on the substrate surface, improving the formation of nanocrystals at low substrate temperature.[22]

There has recently been a report on synthesis of CdS/CdTe nanoparticles by the PLD method to improve the efficiency of cadmium-based solar cells by incorporating nanostructures.[23] However, synthesis of CdS nanowires using PLD has scarcely been reported. In the series of experiments reported herein, crystalline CdS nanoneedles were grown on Ni-coated Si (100) substrates using PLD. The substrate temperature and Ni-catalyst layer thickness were varied to optimize the morphology and crystallinity of the as-grown CdS nanoneedles. Based on the experimental results, the mechanisms of CdS nanoneedle growth are discussed.

EXPERIMENTAL PROCEDURES

CdS nanoneedles were grown on Ni-coated Si (100) substrates by the PLD method. The experimental setup consisted of a Nd:YAG laser with wavelength of 532 nm and a deposition chamber with base pressure of 10^{-4} Pa. Before being placed into the chamber for CdS nanoneedle growth, substrates were first ultrasonically cleaned in acetone and ethanol, then chemically etched in HF solution (H_2O:HF = 3:1), and finally rinsed in deionized

(Received July 6, 2011; accepted February 2, 2012; published online February 24, 2012)

water. Sample preparation involved two steps. In the first step, Ni layers were deposited on the substrates by PLD with laser pulse energy of 50 mJ and repetition rate of 5 Hz, without background gas or substrate heating, for 5 min to 15 min. In the second step, the Ni-coated substrates were first heated to 300°C to 500°C, then CdS nanoneedles were grown by PLD with laser pulse energy of 50 mJ and repetition rate of 10 Hz, without background gas, for 30 min. The morphology of all the samples was examined by field-emission scanning electron microscopy (FESEM) and transmission electron microscopy (TEM). Their crystalline structures were characterized by selected-area electron diffraction (SAED), high-resolution transmission electron microscopy (HRTEM), and x-ray diffraction (XRD). Their room-temperature photoluminescence (PL) spectra were also measured to check the crystallinity and defects.

RESULTS AND DISCUSSION

Different substrate temperatures and Ni-layer thicknesses were tried for growth of CdS nanoneedles. To investigate the effect of substrate temperature on CdS nanoneedle growth, substrate coated by Ni in 10 min predeposition were heated and kept at temperatures between 300°C and 500°C at steps of 50°C during the deposition of CdS nanoneedles. At the 300°C substrate temperature, no nanoneedles had grown after 30 min of CdS deposition, and only a few small tips could be distinguished on the base CdS thin film (Fig. 1a). When the substrate temperature was increased to 350°C, some sparse nanoneedles grew out of the flat, crystalline base CdS thin film (Fig. 1b). In the upper right inset of Fig. 1b, a single nanoneedle with a perfect long triangular-pyramid shape is seen, with middle diameter and length of about 100 nm and 1000 nm, respectively. This may indicate that the Ni layer did not melt at the substrate temperature of 300°C, but began to melt and function as a catalyst at 350°C. As the substrate temperature was further increased, the density of the as-grown nanoneedles increased rapidly. Figure 1c shows the morphology of CdS nanoneedles as grown at 400°C substrate temperature. In Fig. 1c, nanoneedles with long triangular-pyramid shapes can be seen, having average middle diameter and length of 50 nm and 800 nm, respectively, at density of 3.7×10^8 cm^{-2}. With further increase of the substrate temperature to 450°C, dense and randomly oriented nanoneedles grew on the substrate with density of about 1.9×10^9 cm^{-2} (Fig. 1d). These nanoneedles were slightly bent, having average middle diameter and length of 80 nm and 400 nm, respectively. When the substrate temperature was increased to 500°C, again no nanoneedles appeared, and only crystalline blocks grew on the substrate (Fig. 1e).

Figure 2 demonstrates how the Ni-catalyst affects the morphology of the as-grown CdS nanoneedles. Figure 2a presents the morphology of the Ni layer deposited with the 50 mJ/5 Hz pulsed laser for duration of 10 min. It can be seen from Fig. 2a that the Si (100) substrate is covered by Ni nanoparticles with size of 5 nm to 20 nm. Figure 2b–d shows CdS deposited on Ni-covered Si (100) substrate at the same substrate temperature of 400°C for different predeposition durations of Ni-catalyst. As described above, Ni layers melt at substrate temperature of about 400°C. If no Ni-catalyst was deposited prior to the CdS deposition, no nanoneedles grew, and just a flat thin film composed of crystallites with fuzzy appearance grew on the substrate after 30 min of CdS deposition (Fig. 2b). When the Ni predeposition lasted 5 min, still no nanoneedles grew on the substrate, but rather a flat thin film composed of larger crystallites with clear edges (Fig. 2c). On increasing the duration of Ni predeposition to over 10 min, straight CdS nanoneedles were observed to grow out of the base thin film (Fig. 2d).

The crystallinity and growth orientations of the as-grown CdS nanoneedles were determined by SAED, HRTEM, and XRD (Figs. 3, 4). Both samples corresponding to Figs. 3a and 4a were prepared at 400°C substrate temperature and with 10 min of Ni predeposition, being composed of both base crystallites and nanoneedles (Figs. 1c, 2d). The SAED and HRTEM results demonstrate that the nanoneedles grown at 400°C substrate temperature were hexagonal CdS crystals with growth orientation of $\langle 11\bar{2}0 \rangle$ and (0002) lattice spacing of 0.34 nm. The XRD pattern shown in Fig. 4a also verifies the hexagonal structure of the as-grown CdS films.[12] As the (002) peak of CdS is much higher than others such as (103), (212), and (004) of CdS, it can be inferred that the (002) peak of CdS belongs to both the base CdS crystallites and the CdS nanoneedles, while others can be attributed only to the as-grown CdS nanoneedles. The reason for this can be explained as follows: the quantity of base CdS crystallites is much greater than that of the CdS nanoneedles, and the base CdS crystallites have a consistent growth orientation of $\langle 0002 \rangle$, which is perpendicular to the substrate surface, while the CdS nanoneedles are disorderly inclined to the surface of the substrate, although their growth orientations may be the same (Fig. 1c). To prove this interpretation, the XRD pattern of a sample without CdS nanoneedles but only base CdS crystallites (Fig. 2c) was measured, as shown in Fig. 4c. The sample corresponding to Fig. 4c was prepared at 400°C with 5 min of Ni predeposition, and the substrate was partly covered prior to CdS deposition. Therefore, CdS thin film only grew on part of the substrate and the Si peaks can be found in its XRD pattern. In Fig. 4c, excluding the (002) and (004) peaks of cubic Si and two low and wide peaks of amorphous SiO_2, the only obvious peak is attributed to (002) of hexagonal CdS, meaning that the growth orientation of the as-deposited CdS thin film has very good consistency. The two hardly distinguished

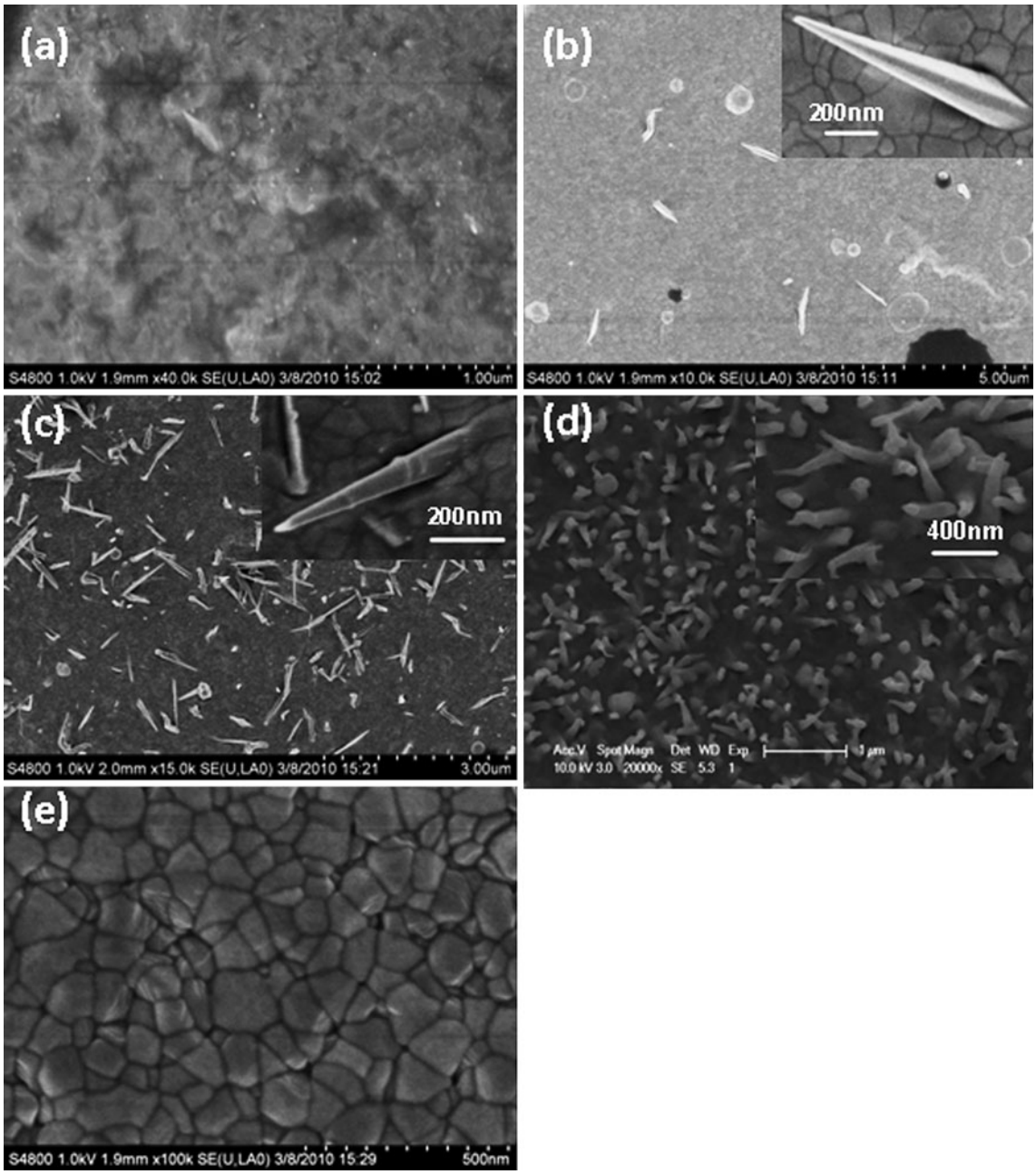

Fig. 1. FESEM images of CdS films grown on Si (100) substrates at different substrate temperatures of (a) 300°C, (b) 350°C, (c) 400°C, (d) 450°C, and (e) 500°C. The duration of Ni-catalyst predeposition was 10 min in all cases, and the laser pulse energy and frequency were 50 mJ and 5 Hz, respectively.

(103) and (203) CdS peaks in Fig. 4c may come from the interface or small nanoneedles covered by base crystallites (described later when discussing the growth modes of the CdS nanoneedles). The room-temperature PL of the sample corresponding to Fig. 1c shows an obvious emission peak at 513 nm, which fits well with the bandgap of bulk CdS (2.42 eV) and indicates that the as-grown CdS thin film has good crystallinity and few defects (Fig. 5).[24]

To further understand the effects of substrate temperature on CdS nanoneedle growth, the crystallinity and orientations of CdS nanoneedles prepared at 450°C substrate temperature and with 10 min of Ni predeposition were also determined by SAED, HRTEM, and XRD (comparing with the sample prepared at the 400°C substrate temperature). Figure 3b shows the TEM morphology of a CdS nanoneedle taken from the sample of Fig. 1d. Its SAED pattern and HRTEM image are shown in the upper right and lower right insets to Fig. 3b, respectively. The HRTEM image and SAED pattern demonstrate that the CdS nanoneedle had good hexagonal crystallinity with growth orientation of $\langle 10\bar{1}0 \rangle$ and (0002) lattice spacing of 0.34 nm. The

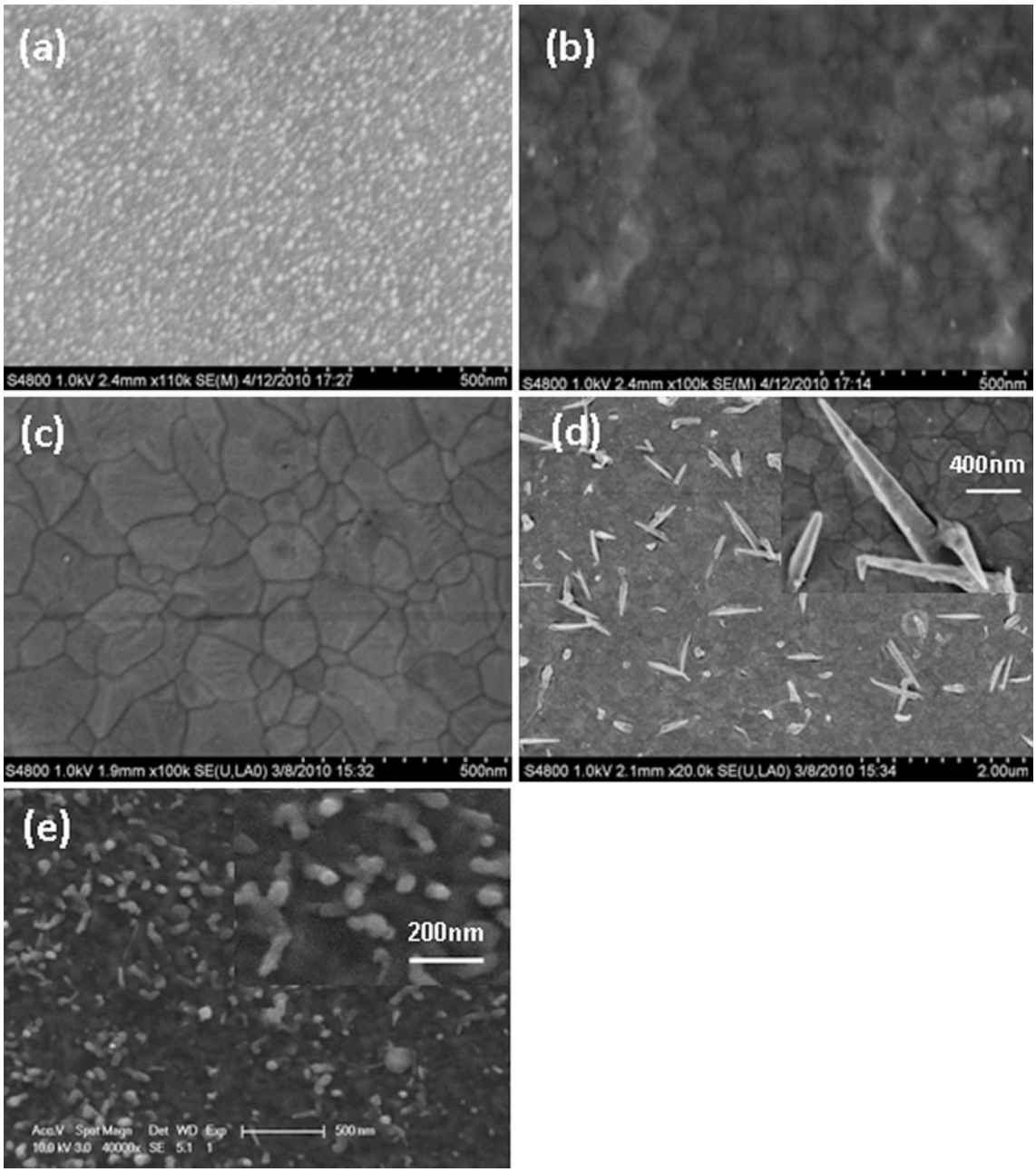

Fig. 2. FESEM images of (a) only the Ni-catalyst layer deposited on bare Si (100) substrate, and (b–e) CdS films grown on Ni-covered Si (100) substrates with different Ni-layer thicknesses. The duration of Ni-catalyst predeposition in (a–e) was 5 min, 0 min, 5 min, 15 min, and 15 min, respectively. Substrate temperatures were (a) room temperature, (b–d) 400°C, and (e) 450°C.

XRD results in Fig. 4b also verify the hexagonal structure of the same as-grown CdS film. As discussed above, the highest peak (002) in Fig. 4b belongs to both the base CdS crystallites and CdS nanoneedles. Besides (103), (212), and (004) peaks of hexagonal CdS appearing in Fig. 4a, there are more peaks such as (100), (101), (102), (110), and (201) of hexagonal CdS appearing in Fig. 4b. It is inferred that the higher density and tip bending of the randomly oriented nanoneedles in Fig. 1d led to the appearance of more hexagonal CdS peaks in the XRD pattern (their growth modes are discussed below).

To understand the mechanism of CdS nanoneedle growth, a cross-section of the sample prepared at 400°C substrate temperature and with 10 min of Ni predeposition was observed by FESEM. Figure 6 shows that CdS nanoneedles grew out of base CdS crystallites and that some small cones were covered by base crystallites at the bottom of the substrate. This can be regarded as a vapor–solid (VS) growth mode (as shown in Fig. 7a).[25] When the feedstock Cd and S atoms generated by laser ablation deposit on the substrate, they form nuclei directly at locations without Ni-catalyst, or dissolve into molten Ni

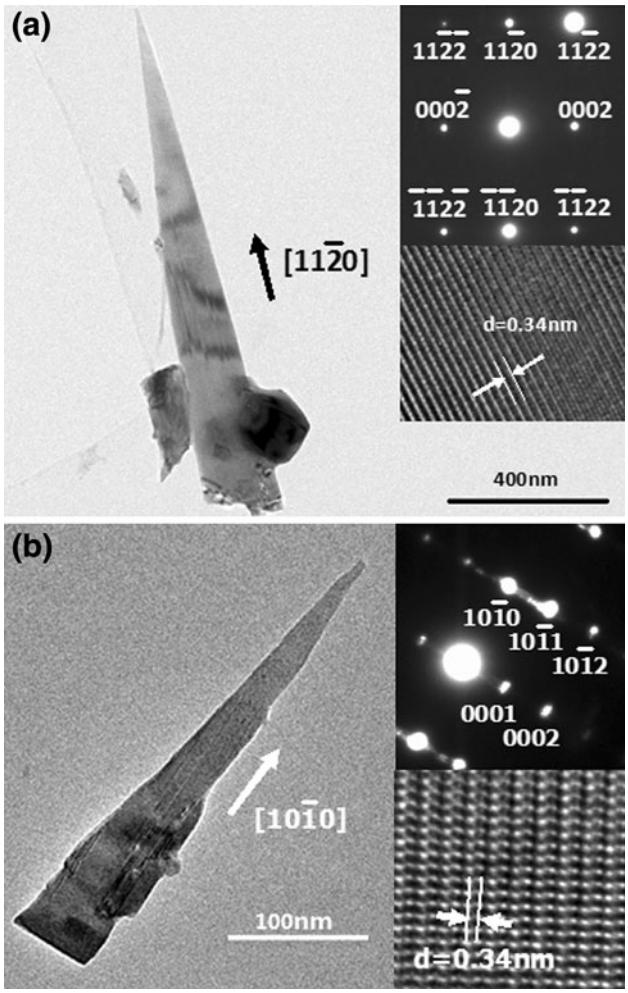

Fig. 3. TEM images of CdS nanoneedles with their SAED patterns in upper right insets and HRTEM images in lower right insets. Both samples were prepared with 10 min of Ni predeposition and at substrate temperature of (a) 400°C (corresponding to the sample in Fig. 1c) and (b) 450°C (corresponding to the sample in Fig. 1d).

spheres if the substrate temperature is appropriate, for example, 400°C. When the dissolution level in the molten Ni spheres becomes supersaturated, the initial CdS sheets separate out onto the molten Ni sphere surface. As more and more ablated Cd and S atoms reach the molten Ni spheres, the separated CdS material will crystallize, and the nuclei of CdS nanoneedles emerging from the melted Ni spheres will be formed. If the primary CdS nanoneedles are high enough, they can grow out of the base crystallites preferentially; otherwise they will be covered by the growing base crystallites and will not grow further.

For higher substrate temperature, the growth of CdS nanoneedles will follow a vapor–liquid–solid (VLS) mode,[17,26] which can help explain the tip bending of the CdS nanoneedles grown at 450°C substrate temperature (Figs. 1d, 2e). For the VLS growth mode, the catalyst spheres are unstable due

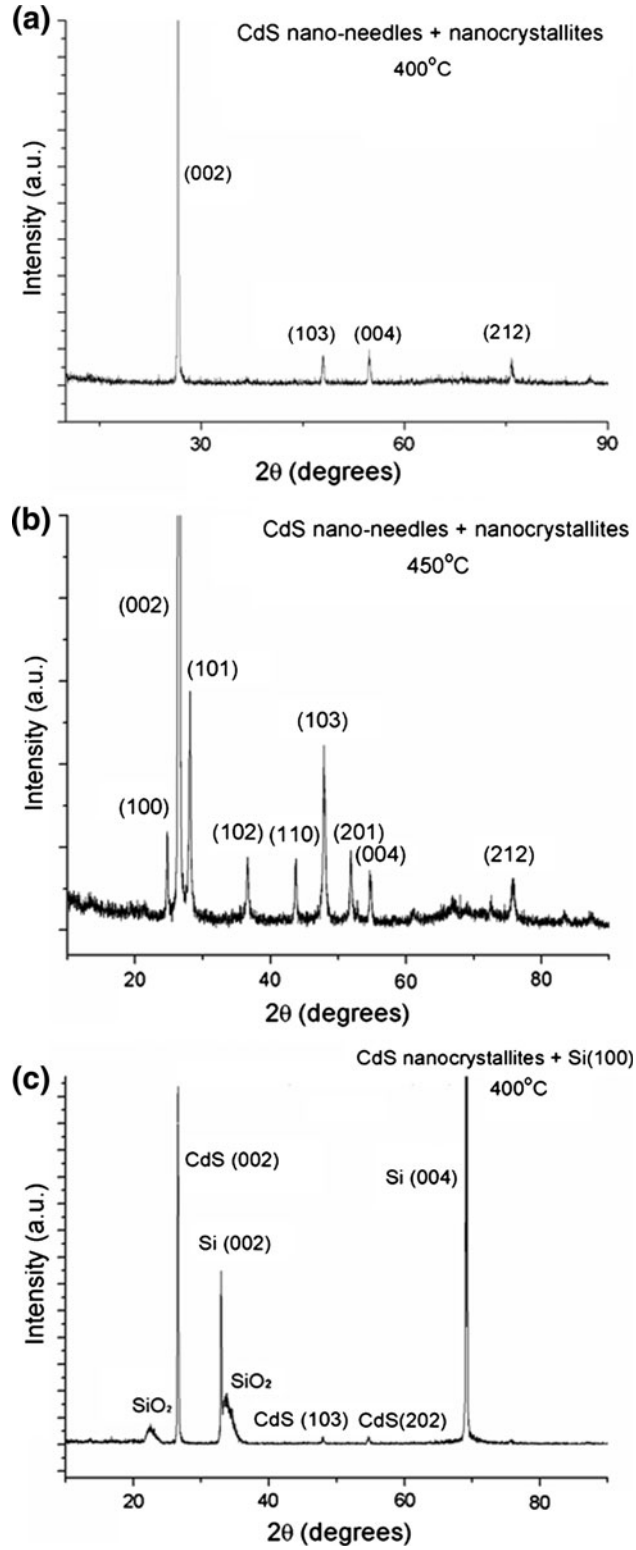

Fig. 4. XRD patterns of (a) uncovered sample prepared at substrate temperature of 400°C and with 10 min of Ni predeposition, (b) uncovered sample prepared at substrate temperature of 450°C and with 10 min of Ni predeposition, and (c) partly covered sample prepared at substrate temperature of 400°C and with 5 min of Ni predeposition.

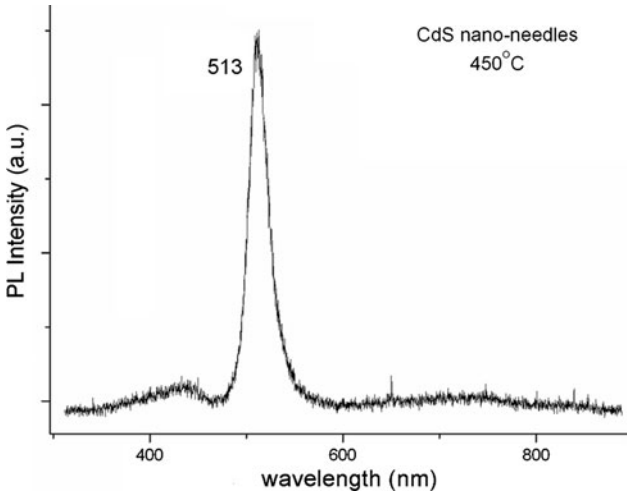

Fig. 5. Room-temperature PL spectrum of the sample (shown in Fig. 1d) prepared at substrate temperature of 450°C and with 10 min of Ni predeposition.

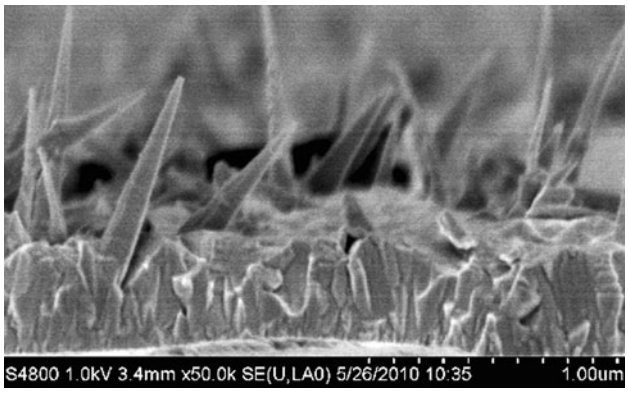

Fig. 6. FESEM image of a cross-section of a sample (as shown in Fig. 1c) prepared at 400°C substrate temperature and with 10 min of Ni predeposition.

to the higher substrate temperature, returning to the substrate surface. The feedstock reaching the unstable catalyst spheres will migrate to their underside, and the initial nuclei of the CdS nanoneedles will emerge below the catalyst spheres. Then, the catalyst spheres will remain on top of the growing nanoneedles, leading to their growth in random directions. Finally, the bent CdS nanoneedles result. As the nanoneedles grow longer, the molten catalyst spheres will solidify due to deficient thermal conductivity to the substrate, and the nanoneedles will suspend growth. Therefore, CdS nanoneedles grown by VLS mode are usually shorter than those grown by VS mode, as shown in Figs. 1 and 2. If the substrate temperature is kept at 450°C and Ni predeposition is prolonged for 15 min, small Ni spheres at the tops of bent nanoneedles are more easily distinguished because of the large quantity of Ni (as shown in Fig. 2e). Figure 7b shows the growth mode for this situation. During VLS growth, the laser-ablated

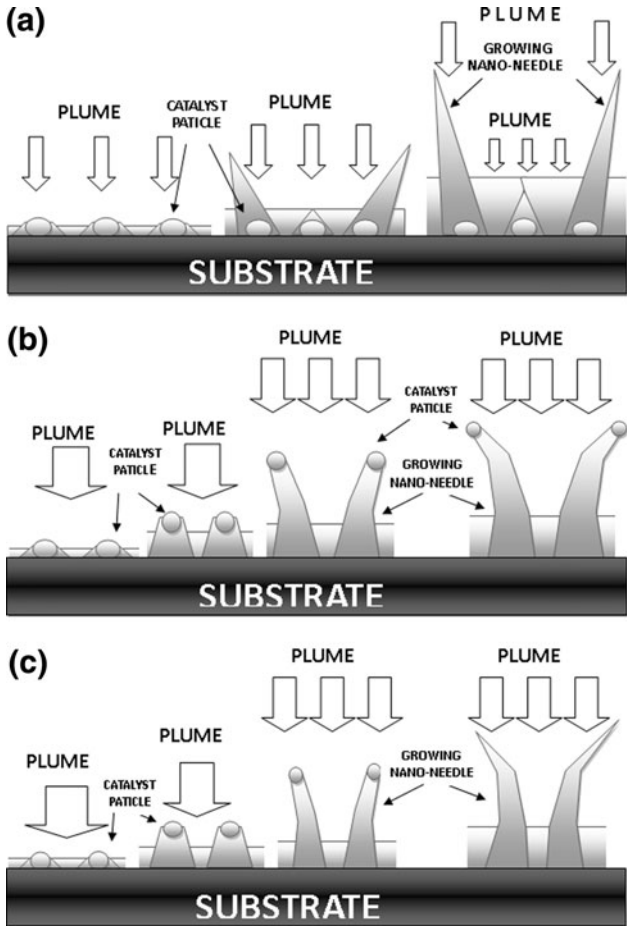

Fig. 7. (a) VS growth mode and (b, c) two types of VLS growth mode of CdS nanoneedles. (b) Ni spheres remain on top of growing CdS nanoneedles. (c) Ni spheres do not remain on top of growing CdS nanoneedles.

plumes with kinetic energy of several to tens of electron volts will act on the catalyst spheres, which may be sputtered off or removed from the tops of the nanoneedles. So, some nanoneedles become sharp due to the removal of the catalyst spheres at the tops (Fig. 1d). Figure 7c demonstrates this kind of growth, in which the molten spheres are removed from the tops of the growing nanoneedles. For lower or higher substrate temperatures (for example, 300°C or 500°C), the catalyst layer will not melt, or molten catalyst islands will be very unstable (strongly moving and jumping), so that CdS nanoneedles will not grow.

CONCLUSIONS

CdS nanoneedles have been grown on Ni-coated Si (100) substrates by the PLD method. The substrate temperature and predeposited Ni-catalyst layer thickness strongly affect the growth of the CdS nanoneedles. If the substrate temperature is kept at around 400°C, CdS nanoneedles with good shape can grow out of the base CdS crystallites via the VS mode. These CdS nanoneedles have average middle diameter and length of 50 nm and 800 nm,

respectively, and density of about 10^8 cm^{-2}. When the substrate temperature is set at 450°C, the bent CdS nanoneedles are led by a Ni sphere, having average middle diameter and length of 80 nm and 400 nm, respectively, and density of about 10^9 cm^{-2} and growing by the VLS mode. The CdS nanoneedles grown by both growth modes have perfect hexagonal crystallinity, and the base CdS crystallite layers also have hexagonal crystallinity and orientation consistency. Such good crystallinity makes the CdS nanoneedles a channel for electron transport. The large specific surface areas of the CdS nanoneedles will increase the interfaces of *p–n* junctions to improve device efficiency and sensitivity. For hybrid solar cells, the large specific surface area of the CdS nanoneedles will enhance the separation of nearby excitons to produce more electrons and holes. Also, dense nanowires can increase the absorption of photons when light travels in the film. The good crystallinity and large specific surface area of the CdS nanoneedles grown by PLD indicate that they have potential for application in highly efficient CdS-related LEDs, sensors, hybrid solar cells, and other photoelectronic devices. In addition, the dense base CdS crystallite layers of the prepared samples can effectively isolate the functional layers from the substrates, which is beneficial for fabrication of CdS-based devices. The room-temperature PL of the prepared samples shows an obvious emission peak at 513 nm, corresponding to the bandgap of 2.42 eV, being located near the strongest band in the solar spectrum, revealing that such as-grown CdS nanoneedles have potential for application in hybrid solar cells.

ACKNOWLEDGEMENTS

The authors acknowledge the support from the National Basic Research Program of China (973 Program) (Grant No. 2010CB933703) and National Natural Science Foundation of China (Grant No. 10875030).

REFERENCES

1. X.Z. Wu, *Sol. Energy* 77, 803 (2004).
2. A. Morales-Acevedo, *Sol. Energy* 80, 675 (2006).
3. N.D. Kumar, M.P. Joshi, C.S. Friend, P.N. Prasad, and R. Burzynski, *Appl. Phys. Lett.* 71, 1388 (1997).
4. J.L. Zhao, J.A. Bardecker, A.M. Munro, M.S. Liu, Y.H. Niu, I.-K. Ding, J.D. Luo, B.Q. Chen, A.K.-Y. Jen, and D.S. Ginger, *Nano Lett.* 6, 463 (2006).
5. V. Smyntyna, V. Golovanov, S. Kačiulis, G. Mattogno, and G. Righini, *Sens. Actuat. B* 25, 628 (1995).
6. Y.R. Roh, H.B. Kim, Y.J. Lee, H.M. Cho, J.S. Chung, and S. Baik, *Proc. IEEE Ultrason. Symp.* 1, 473 (1995).
7. J.N. Ross, *Meas. Sci. Technol.* 6, 405 (1995).
8. J.S. Jang, W. Li, S.H. Oh, and J.S. Lee, *Chem. Phys. Lett.* 425, 278 (2006).
9. K.G. Kanade, J.-O. Baeg, U.P. Mulik, D.P. Amalnerkar, and B.B. Kale, *Mater. Res. Bull.* 41, 2219 (2006).
10. J.-C. Lee, W. Lee, S.-H. Han, T.G. Kim, and Y.-M. Sung, *Electrochem. Commun.* 11, 231 (2009).
11. D.S. Xu, Y.J. Xu, D.P. Chen, G.L. Guo, L.L. Gui, and Y.Q. Tang, *Adv. Mater.* 12, 520 (2000).
12. D. Routkevitch, T. Bigioni, M. Moskovits, and J.M. Xu, *J. Phys. Chem.* 100, 14037 (1996).
13. J.S. Suh and J.S. Lee, *Chem. Phys. Lett.* 281, 384 (1997).
14. J. Yang, J.H. Zeng, S.H. Yu, L. Yang, G.E. Zhou, and Y.T. Qian, *Chem. Mater.* 12, 3259 (2000).
15. Y.D. Li, H.W. Liao, Y. Ding, Y.T. Qian, L. Yang, and G.E. Zhou, *Chem. Mater.* 10, 2301 (1998).
16. X.L. Shi, M.S. Cao, J. Yuan, Q.L. Zhao, Y.Q. Kang, X.Y. Fang, and Y.J. Chen, *Appl. Phys. Lett.* 93, 183118 (2008).
17. Y.W. Wang, G.W. Meng, L.D. Zhang, C.H. Liang, and J. Zhang, *Chem. Mater.* 14, 1773 (2002).
18. X.F. Duan and C.M. Lieber, *Adv. Mater.* 12, 298 (2000).
19. T. Yoshitake, T. Nagamoto, and K. Nagayama, *Thin Solid Films* 381, 236 (2001).
20. Y.R. Ryu, S. Zhu, S.W. Han, H.W. White, P.F. Miceli, and H.R. Chandrasekhar, *Appl. Surf. Sci.* 128, 496 (1998).
21. J.W. Park, C.M. Rouleau, and D.H. Lowndes, *J. Cryst. Growth* 193, 516 (1998).
22. J.P. Zheng, Z.Q. Huang, D.T. Shaw, and H.S. Kwok, *Appl. Phys. Lett.* 54, 280 (1989).
23. A. Bylica, P. Sagan, I. Virt, G. Wisz, M. Bester, I. Stefaniuk, and M. Kuzma, *Thin Solid Films* 512, 439 (2006).
24. D. Kulik, H. Htoon, and C.K. Shih, *J. Appl. Phys.* 95, 1056 (2004).
25. J.S. Lee, S. Brittman, D. Yu, and H.K. Park, *J. Am. Chem. Soc.* 130, 6252 (2008).
26. J.S. Lai, L. Chen, X.N. Fu, J. Sun, Z.F. Ying, J.D. Wu, and N. Xu, *Appl. Phys. A* 102, 477 (2010).